

PROGRESSIVE FAILURE IN GLASS FIBRE REINFORCED POLYMER COMPOSITES

R. K. Joki^{1,2*}, F. Grytten¹, H. Osnes²

¹SINTEF, Materials & Chemistry, Pb 124 Blindern, NO-0314 Oslo, Norway

²Mechanics div, Dep. Mathematics, University of Oslo, Pb 1053 Blindern, NO-0316 Oslo, Norway

*reidar.joki@sintef.no

Keywords: Failure criteria, progressive damage, plane stress, FEM

Abstract

This study addresses the nonlinear stress-strain response in glass fibre reinforced polymer composite laminates subjected to in-plane loading. A user defined material model is implemented in the finite element code LS-DYNA. The model is calibrated and evaluated using results from a large material testing survey. Failure theory as well as the damage evolution is based on the Puck failure criterion. The constitutive model treats the mix of fibre and matrix as homogeneous and anisotropic, whereas failure is either associated with the fibres or the polymer matrix. The progressive damage is initiated by matrix failure, and treated as a smeared degradation of the lamina properties. The laminates are modelled using both shell and solid elements. The benefits of using solid elements are shown to be small compared to the severe increase in computational cost.

1 Introduction

Fibre Reinforced Polymer Composite materials (FRPC) are more complex than classical materials such as metals. They are heterogeneous and anisotropic, with strength and stiffness in the direction parallel to the fibres being several times greater than in the transverse direction. A major challenge when analysing the mechanical properties of FRPC is the prediction of failure due to a specified state of stress. The micro structural aspect of failure makes it difficult to provide models that are easy to calibrate, produce accurate results and are robust with respect to loading conditions and element size and shape.

A common assumption or simplification made in the literature covering failure in this type of composites, is that they are brittle with little or no ability for plastic deformation [1]. Non-linear stress-strain response has therefore been treated as damage. Damage refers to the more or less gradual developments of micro cracks in the matrix material which leads to macro cracks and then finally to ultimate failure caused by fibre failure. Plastic deformation or other causes for irreversible deformation are excluded from this type of models. All nonlinearity in the stress-strain relation is caused by reduction of secant stiffness, which means that when a simulated model is unloaded after loading beyond failure initiation, it will return to its initial geometry without residual stresses.

A common use of FRPC is laminates of plies or laminas with unidirectional fibres. A laminate can have plies with various orientations. The analysis of progressive failure in these laminates can be divided into two aspects; the first being the identification of failure initiation, the

second being the degradation of the material properties when loaded past failure initiation. The first aspect can be divided into two categories; intra lamina failure describing response within the laminae, and inter lamina failure which address the interaction between the laminae. This study addresses the first category. Intra lamina failure prediction has been the goal for a lot of work published in the last 40 years. Some of these works have been widely used in both research and industry; The Tsai-Wu [2], the Hashin [3] and the Puck [1] failure criterion, to mention just a few. In 2004 the World Wide Failure Exercise [4] was published. This book covers 12 years of coordinated international work with the aim of bringing together all of the results, encompassing 19 failure theories, and assessing them together in a single volume. The Puck failure criterion was ranked as one of the most promising. Classical failure criteria such as the Tsai-Wu criterion were derived at a time when computational capacity was a scarce resource, and therefore depended on an analytical solution and a less detailed input for it to be practical in use. The boost in computational capacity has opened for criteria such as the Puck criterion which is a physically based phenomenological model.

When basing a numerical model on the theory described above, it is reasonable to build a constitutive model for a single ply, and then rotate this constitutive model to capture the various ply orientations through the thickness of the laminate. There are several available methods of modelling a laminate of such plies in most finite element codes. One approach is to model each ply with solid elements, and then define the orientation of the constitutive model within each layer of elements. Another approach is to use shell elements with through-thickness integration points for each ply in the laminate. The latter is a well-known method for saving computational costs, but may also add nonphysical stiffness to the model because of constraints on shear deformation.

2 The Puck failure criterion

The Puck failure criterion is applicable to composite laminates containing unidirectional plies. The plies are assumed to be transversely isotropic and the anisotropy is defined by Cartesian coordinate axes, with 1-direction being in the direction parallel to the fibres, 2-direction being the orthogonal in-plane direction, and the 3-direction defines the ply normal. The plane of isotropy is defined by the 2- and 3-axes.

2.1 Fibre failure

It is assumed that there is a perfect adhesion between fibre and matrix, i.e. the strain parallel to the fibres (ϵ_{11}) is the same for both fibres (ϵ_{f1}) and matrix (ϵ_{m1}): $\epsilon_{f1} = \epsilon_{m1}$. During combined loading the strain in the fibres will be:

$$\epsilon_{f1} = \frac{\sigma_{f1}}{E_{f1}} - \frac{\nu_{f12}}{E_{f1}} m_{\sigma f} \sigma_{22}, \quad (1)$$

where ν_{f12} is the Poisson's ratio for the fibres, and $m_{\sigma f}$ accounts for the stress magnification effect (for glass fibre $m_{\sigma f} \approx 1.3$, and for carbon fibre $m_{\sigma f} \approx 1.1$ [1]) caused by the different moduli of matrix and fibres, which leads to a non uniform distribution of σ_{22} from a microscopic point of view. Thus the fibre failure criterion for tension in the fibre is given by:

$$\frac{1}{\epsilon_{1T}} \left(\epsilon_{11} + \frac{\nu_{f12}}{E_{f1}} m_{\sigma f} \sigma_{22} \right) = 1 \text{ for } (...) \geq 1, \quad (2)$$

where ϵ_{1T} is the ultimate tensile strain in the longitudinal direction. A shear correction factor is included in the original Puck fibre failure criterion. In the present study, it has been observed that the shear correction factor leads to FF although no compressive stress was present in the fibre direction. Therefore the following expression, without the shear correction factor, has been implemented and applied her inn:

$$\frac{1}{\epsilon_{1C}} \left| \left(\epsilon_{11} + \frac{\nu_{f12}}{E_{f1}} m_{\sigma f} \sigma_{22} \right) \right| = 1 \text{ for } (...) < 1, \quad (3)$$

where ϵ_{1C} is the ultimate compressive strain in the longitudinal direction.

2.2 Inter fibre failure

The Puck failure criterion has an analytical solution for plane stress conditions [1]. When taking into account out of plane effects, i.e. through the thickness shear stress, and loading conditions in three dimensions, the Puck Inter Fibre Failure (IFF) criterion has no analytical solution. A full 3-D formulation of the Puck IFF criterion was used by Wigand et al. [5], and has the formula:

$$e^2 = \begin{cases} \left(\frac{\sigma_n}{R_n} \right)^2 + \left(\frac{\tau_{n1}}{R_{n1} - p_{n1}\sigma_n} \right)^2 + \left(\frac{\tau_{nt}}{R_{nt} - p_{nt}\sigma_n} \right)^2, & \text{for } \sigma_n \geq 0 \\ \left(\frac{\tau_{n1}}{R_{n1} - p_{n1}\sigma_n} \right)^2 + \left(\frac{\tau_{nt}}{R_{nt} - p_{nt}\sigma_n} \right)^2, & \text{for } \sigma_n < 0, \end{cases} \quad (4)$$

where the stress components σ_n , τ_{n1} and τ_{nt} are the stresses acting on the fracture surface as illustrated in Figure 1 and defined by the angle of the fracture surface, θ_{fp} , in Equation (5). The parameter R_n describes the resistance of the fracture plane against normal failure induced by σ_n . The parameters R_{n1} and R_{nt} are the resistance of the fracture plane against shear, and finally, p_{n1} and p_{nt} are the slope parameters representing internal friction effects [5]. Puck suggests the values presented in Equation (6) for these parameters [6].

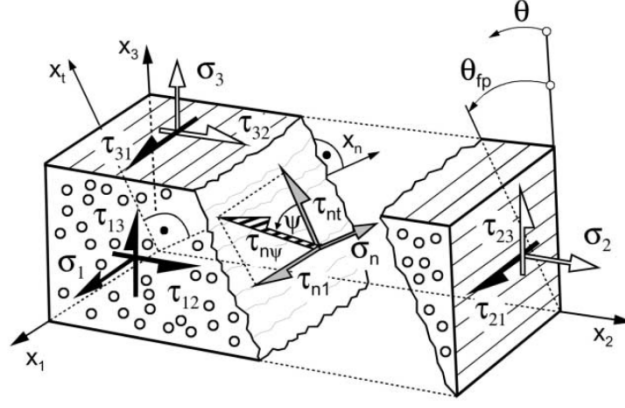


Figure 1: Illustration of the fracture surface and the stress components acting on the surface [6].

$$\begin{aligned}
 \sigma_n &= \sigma_{22} \cos^2 \theta_{fp} + \sigma_{33} \sin^2 \theta_{fp} + 2\sigma_{23} \cos \theta_{fp} \sin \theta_{fp}, \\
 \tau_{n1} &= \sigma_{12} \cos \theta_{fp} + \sigma_{13} \sin \theta_{fp}, \\
 \tau_{nt} &= -\sigma_{22} \sin \theta_{fp} \cos \theta_{fp} + \sigma_{33} \sin \theta_{fp} \cos \theta_{fp} + \sigma_{23} (\cos^2 \theta_{fp} - \sin^2 \theta_{fp}).
 \end{aligned} \tag{5}$$

$$\begin{aligned}
 R_n &= S_{22}^+, \\
 R_{n1} &= S_{12}, \\
 R_{nt} &= \frac{S_{22}^-}{2 \tan(\theta_{fp}^0)}, \\
 p_{nt} &= -\frac{1}{\tan(2\theta_{fp}^0)}, \\
 p_{n1} &= p_{nt} \frac{R_{n1}}{R_{nt}}.
 \end{aligned} \tag{6}$$

Here, S_{22}^+ and S_{22}^- are the transverse strengths in tension and compression, respectively, and S_{12} is the shear strength. The angle θ_{fp}^0 is the angle at which a specimen loaded in uniaxial compression in the transverse fibre direction fracture due to shear failure. When subjected to in-plane loading, IFF is provoked by σ_{22} and τ_{12} . The shape of the failure envelope depends strongly on θ_{fp}^0 , especially for the interpolation between in-plane shear and compressive transverse loading. This angle can be looked upon as a material property and has a constant value for a given material. It should be emphasised that this is not the same angle as the fracture angle defining the action plane of an arbitrary loading condition θ_{fp} .

Because no analytical solution to the criterion exists, one needs to search through all the possible failure planes to find the one where the parameter e has its maximum value. The criterion is defined by the failure surface stress components σ_n , τ_{n1} and τ_{nt} , and consequently they have to be calculated for every search angle. Because of symmetry, the

search for the critical action plane can be limited to the range $-90^\circ \geq \theta \geq 90^\circ$. CPU-costs may be decreased by using a good search algorithm. The Golden Section Search has been shown to be effective in the search for the action plane by Wiegand et al. [5].

3 Progressive failure

The strength parameters found in the IFF criterion (S_{22}^+ , S_{22}^- and S_{12}) represent the end of the linearity in the stress-strain response. The reasons for this non-linearity are plastic and viscoelastic behaviour of the matrix and, probably above all, micro-damage [7]. Typically a micro crack in the matrix will propagate until it is stopped by a crossing fibre. At the location of the micro-damage, the stiffness of the matrix is reduced to zero, while the rest of the matrix material holds the initial stiffness. As more and more of these micro cracks develop, the overall global stiffness will be degraded in a progressive manner. The development of these micro-cracks will affect the global transverse stiffness E_{22} and E_{33} , the shear stiffness G_{12} , G_{13} and G_{23} , as well as the Poisson's ratios ν_{12} , ν_{13} and ν_{23} . It is reasonable to address the development of micro-damage as smeared, and multiply E_{22} , E_{33} , G_{12} , G_{13} , ν_{12} , ν_{13} and ν_{23} with a progressive reduction factor. Puck argues that these material properties may be reduced concurrently by the same reduction factor, η [7]. Puck also argues that the following expression is a reasonable approximation to this reduction factor:

$$\eta = \begin{cases} 1 & , \text{ for } f_{E(IFF)} < 1 \\ \frac{1-\eta_r}{1+c(f_{E(IFF)}-1)^\xi} + \eta_r & , \text{ for } f_{E(IFF)} \geq 1, \end{cases} \quad (7)$$

where the dimensionless parameters c and ξ serve to fit the η -curve to experimental results. The term η_r represents a small remaining stiffness ($\eta_r < 1$). The values of c , ξ and η_r have been determined using the optimisation code LS-OPT. The simulated response has been fitted to experimental results from tensile loading of 6-layered laminates with 5% of the fibres in each layer in the longitudinal direction and 95% in the transverse direction. It is assumed that the 5% of the fibres that are oriented in the longitudinal direction behave elastically until failure.

4 Material tests

All the material properties used to describe the elastic behaviour are based on an extensive material testing exercise using low strain rates. The tensile, compressive and shear tests are carried out in accordance to the ASTM D3039, D6641, D 3518 and ASTM D7078. Seven different laminate lay-ups have been tested $[0]_6$, $[90]_6$, $[0/90]_6$, $[\pm 45]_6$, $[0/45/90/-45]_6$, $[\pm 45/(0)_6/\pm 45]$ and $[\pm 45/(90)_6/\pm 45]$, where the numbers within the brackets indicate the orientation of the longitudinal ply direction with respect to the loading direction, the order of the numbers indicate the stacking sequence and the subscript how many times the sequence is repeated through the laminate. All the deduced material properties are displayed in Table 1, with the elastic properties in the left column, the strength properties in the centre column, and finally the properties specially needed for the Puck failure criterion in the column on the right. The fracture angle for pure transverse compression, θ_{fp} , is obtained from literature for an equivalent material. The reduction factor η was calibrated by evaluating the response in $[90]_6$ -laminates, which represents the reduction in transverse stiffness.

Elastic Properties			Strength Properties			Puck Failure Criterion	
E_{11}	42028	MPa	S_{11}^+	1100	MPa	θ_{ip}^0	51
E_{22}	11472	MPa	S_{11}^-	600	MPa	E_{1f}^+	73000 MPa
G_{12}	4000	MPa	S_{22}^+	28	MPa	ν_{1f}	0.20
ν_{12}	0.25		S_{22}^-	200	MPa	c	0.527
ν_{23}	0.30		S_{12}	50	MPa	η_r	0.034
			S_{23}	50	MPa	ξ	1.670

Table 1. Material properties

5 Finite element modelling

All the simulations presented here are carried out using the implicit solver in LS-DYNA with a user defined material model. The material model has been tested to work well with both implicit and explicit analysis.

The thicknesses of the plies in a laminate are thin compared to their width and length. When using solid elements, the aspect ratios should be kept as close to unity as possible. Large aspect ratios may cause locking or numerical instability. The element size is therefore generally dictated by the thickness of the plies when modelling the laminate using solid elements, leaving the model with a high number of elements and consequently being more computational expensive than when using shell elements. To reduce the computational cost of the model, only a quarter of the test specimen is modelled due to symmetry, as is illustrated in Figure 2. Note that due to off-axis loading of lamina and through thickness shear deformations, the sample will in reality not behave symmetrically about the indicated symmetry planes. However, it is assumed to be a reasonable simplification.

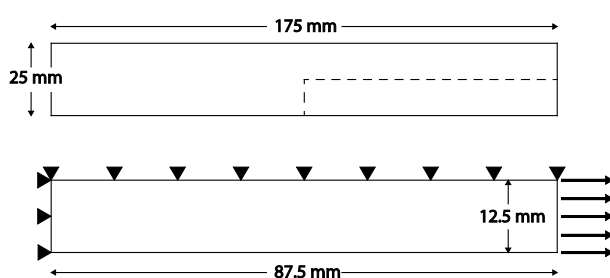


Figure 2. Top: The specimen geometry. Bottom: model geometry.

6 Results

The response of three laminates have been investigated, these are $[90/-45/45]_6$, $[0/45/90/-45]_6$ and $[45/-45/(90)_6/45/-45]$. The results are listed in Table 2 and displayed in Figure 3, 4 and 5. The experimental results are obtained in accordance with the ASTM D3039 test standard. Numerical results are obtained using both shell and solid elements.

Property	Experimental	Shell elements	Solid elements
[90/-45/45]₆			
Average cpu time pr. strain incr. (s)	--	7.96	101.9
Strain at end of linear response (%)	0.30	0.25	0.25
Nom stress at 2 % strain (MPa)	114	123	120
[0/45/90/-45]₆			
Average cpu time pr. strain incr. (s)	--	19.58	348.8
Strain at end of linear response (%)	0.40	0.40	0.40
Nom stress at 2 % strain (MPa)	318	332	330
[45/-45/(90)₆/45/-45]			
Average cpu time pr. strain incr. (s)	--	14.00	1451.2
Strain at end of linear response (%)	0.25	0.25	0.25
Nom stress at 2 % strain (MPa)	92	126	118

Table 2. Comparing experiments and simulations.

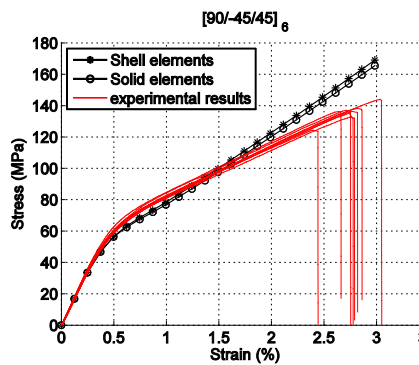


Figure 3. Stress strain response in [90/-45/45]₆-laminates.

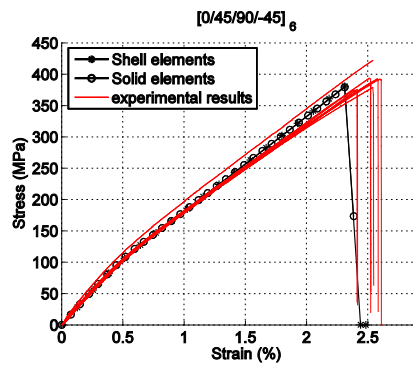


Figure 4. Stress strain response in [0/45/90/-45]₆-laminates.

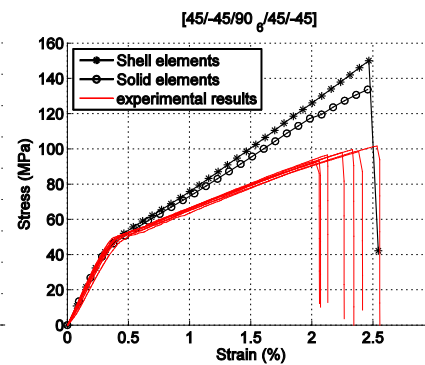


Figure 5. Stress strain response in [45/-45/(90)₆/45/-45]-laminates.

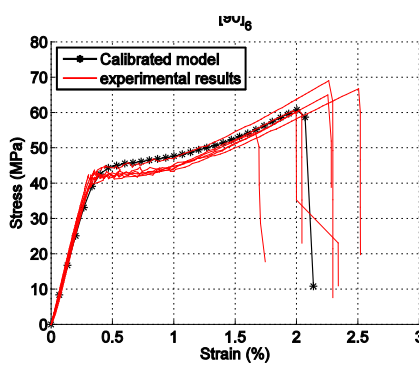


Figure 6. Transverse response.

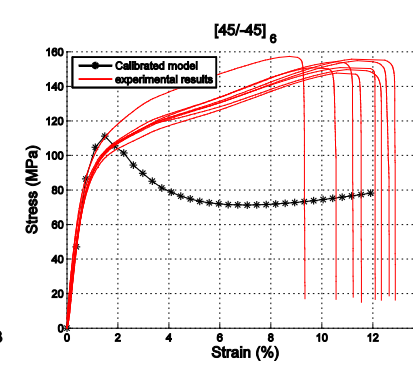


Figure 7. Shear response.

7 Discussion

Puck et al. [1] argues that shear and transverse stiffness can be degraded using the same reduction factor η . This assumption does not agree with the material tests evaluated in this study. The reduction factor used in this study was optimized to fit the stress strain response of

[90]₆-laminates, which represent an isolation of the transverse response (see Figure 6). When used to simulate the response of [45/-45]₆-laminates, representing the shear response, the softening in the stress strain response did not fit the experimental results (see Figure 7). When the [45/-45]₆-laminates were used as optimization fit for the reduction factor, the model failed to fit the experimental results from the [90]₆-laminates. It seems separate reduction factors should be defined for shear and transverse properties.

The results presented in Table 2 and Figure 3, 4 and 5, are from laminates containing both transverse and shear response. Both first ply failure and the progression of damage is well represented by both shell and solid elements. The responses are somewhat stiffer when using shell elements than when using solid elements, but the difference is close to negligible. It is reasonable to expect the difference to be larger if the loading conditions had introduced bending moments in addition to in-plane stress. The increase in simulation time when using solid elements instead of shell elements is quite extensive, compared to the change in the stress strain response.

8 Conclusion

The implemented material model produces acceptable results for in-plane loading conditions. The added accuracy when modelling the laminates using solid elements does not justify the increase in computational cost.

9 Acknowledgment

This work is part of the collaborative project "Composite structures under impact loading" with the industrial partners Flowtite Technology AS, Nammo Raufoss AS, Ragasco AS and the research institutes Norwegian University of Science and Technology (NTNU), University of Oslo (UiO), SINTEF Materials and Chemistry and SINTEF Raufoss Manufacturing. The authors would like to express their thanks for the financial support by the Norwegian Research Council (grant 193238/i40) and the industrial partners. The authors would also like to thank all partners in the project for constructive discussions.

References

- [1] A. Puck and H. Schürmann, Failure Analysis of FRP Laminates by Means of Physically Based Phenomenological Models, *Composites Science and Technology*, vol. 58, pp. 1045-1067, 1998.
- [2] S. W. Tsai and E. M. Wu, A General Theory of Strength for Anisotropic Materials, *J. Comp. Mater.*, vol. 5, pp. 58-80, 1971.
- [3] Z. Hashin, Failure Criteria for Unidirectional Fibre Composites, *Journal of Applied Mechanics*, vol. 47, pp. 329-334, 1980.
- [4] M. J. Hinton, et al., *Failure Criteria in Fibre Reinforced Polymer Composites: The World-Wide Failure Exercise*: Elsevier, 2004.
- [5] J. Wiegand, et al., An algorithm for determination of the fracture angle for the three-dimensional Puck matrix failure criterion for UD composites, *Composites Science and Technology*, vol. 68, pp. 2511-2517, 2008.
- [6] A. Puck, et al., Guidelines for the determination of the parameters in Puck's action plane strength criterion, *Composites Science and Technology*, vol. 62, pp. 371-378, 2002.
- [7] A. Puck and H. Schürmann, Failure analysis of FRP laminates by means of physically based phenomenological models, *Composites Science and Technology*, vol. 62, pp. 1633-1662, 2002.